Supporting Information for

Red CPL from water insoluble achiral carbon dots assisted by cyclodextrin MOF Templating

Ning Feng, [†] [a, c] Xinyi Cai [†] [b, c], Boxin Ding [a], Hongguang Li [*c], and Hong Meng[*a]

[a] Peking University Shenzhen Graduate School, Peking University, Shenzhen 518055, China

[b] College of Chemistry and Molecular Engineering, Peking University, Beijing 100871, China

[c] Key Laboratory of Special Functional Aggregated Materials and Key Laboratory of Colloid and Interface Chemistry, Ministry of Education, School of Chemistry and Chemical Engineering, Shandong University, Jinan 250100, China

[†] These authors contribute equally.

Corresponding Author

Hong Meng: menghong@pkusz.edu.cn Tel: +86 185 6580 7998

Hongguang Li: hgli@sdu.edu.cn Tel: +86 531 88363963

1. Experimental section

1.1 Reagent

1,8-Diaminonaphthalene, sodium lignosulfonate (LIG), and potassium chloride (KCl) were purchased from Macklin Reagent Co., Ltd.; ethanol, N, N-dimethylformamide (DMF), and methanol were purchased from Sinopharm Chemical Reagent Co., Ltd.; γ-cyclodextrin (CyD) was purchased from Sigma-Aldrich Reagent Company. Considering that LIG is a non-stoichiometric complex mixture, elemental analysis of the purchased LIG was performed, revealing carbon, nitrogen, and sulfur contents of 28.73%, 0.74%, and 2.70%, respectively.

1.2 Preparation of Red-Emissive CDs

For DL-CDs, 1.00 g of LIG and 1.00 g of diaminonaphthalene were weighed into the quartz liner of an autoclave, followed by the addition of 75 mL of anhydrous ethanol to dissolve the reagents. The quartz liner was placed in the autoclave, which was then heated to 200 °C with mechanical stirring for 6 h. After natural cooling to room temperature, crude red-emissive CDs were obtained. For DN-CDs, the above procedure was followed but omitting the addition of LIG.

To purify the crude product, approximately 30 mL of anhydrous ethanol was added to the reaction solution, followed by stirring and filtration to collect the filtrate. Subsequently, ~300 mL of deionized water was added to the filtrate, and the mixture was allowed to stand for ~12 h. The resulting suspension was transferred to a 50 mL centrifuge tube, centrifuged at 8000 r min^{-1} for 8 min, and the supernatant was decanted. The obtained solid was dissolved in DMF, filtered again to collect the filtrate, and the filtrate was then transferred to a 1000 Da dialysis bag for dialysis against pure water for 3-4 days. Finally, the dialyzed solution was transferred to a 50 mL centrifuge tube and lyophilized to yield purified CDs solid powder.

5.2.3 Preparation of MOFs and Composite Materials

0.163 g of CyD and 0.0746 g of KCl were weighed into an open weighing bottle. A specified volume of deionized water was added, followed by the CDs DMF solution. The bottle was sealed with parafilm, sonicated for ~10 min, and the final mixture (total volume: 5 mL) was designated as the carbon dot-containing solution for CD@*i*CK-MOF preparation. At this point, the CDs concentration and DMF content of the precursor solution are recorded. A large beaker was filled with ~50 mL of methanol, and the weighing bottle was placed in its center. The beaker was sealed and stored in a 20 °C thermostatic incubator for 4 days. Afterward, the supernatant was poured off, and the bottle was inverted and dried in a fume hood for 2 days to obtain CD@*i*CK-MOF solid particles. *i*CK-MOF was prepared by replacing the CDs DMF solution in the above procedure with pure DMF.

5.2.4 Structural Characterization and Optical Measurements

High-resolution transmission electron microscopy (HR-TEM) images were recorded using a JEM-2100 microscope (JEOL, Japan). For sample preparation, CDs were dissolved in DMF to prepare a 0.1 mg mL^{-1} solution, which was drop-cast onto a pure carbon-supported copper grid and dried under an infrared lamp for 1 h. Raman spectra were collected on a LabRAM HR Evolution in-situ confocal micro-Raman spectrometer (Horiba, Japan) by irradiating sample areas on glass slides with a 325 nm laser. Thermogravimetric analysis (TGA) was performed on a TGA-5500 high-precision thermogravimetric analyzer (TA Instruments, USA) under a N_2 atmosphere with a heating rate of 10 °C min^{-1}. Fourier-transform infrared (FT-IR) spectra were acquired using a Tensor II FT-IR spectrometer (Bruker, Germany) with KBr pellets. UV-Vis absorption spectra were measured on a Cary 5000 spectrophotometer (Agilent, USA). Fluorescence spectra were recorded on a FluoroMax-4 fluorometer (Horiba, Japan), a 510 nm filter (50% transmittance) was used. Quantum yields and fluorescence lifetimes were determined using an FLS920/LP 920 time-resolved molecular spectroscopy system (Edinburgh Instruments, UK). Circularly polarized luminescence (CPL) spectra were measured on a CPL-300 circularly polarized luminescence spectrometer (JASCO, Japan). Single crystals of *i*CK-MOF with suitable dimensions were chosen under an optical microscope. The crystal was mounted on a CryoLoop™ loop and the cell parameters and intensity data were recorded on a Rigaku Oxford Diffraction XtaLAB Synergy-S diffractometer equipped with a HyPix-6000HE Hybrid Photon Counting (HPC) detector operating in shutterless mode and an Oxford Cryosystems Cryostream 800 Plus at 100 K using Cu Kα (λ = 1.54184 Å) PhotonJet micro-focus X-ray Source. Data were processed using the CrystAlisPro software suite.

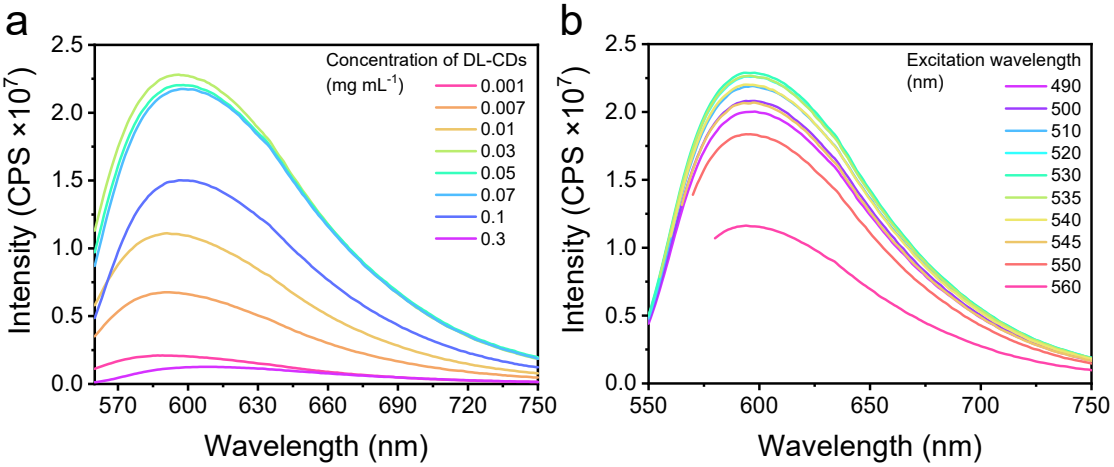

Fig. S1 PL spectra of DL-CDs: (a) concentration dependence (λ_{ex}=530 nm), (b) excitation wavelength dependence (0.03 mg mL^{-1})

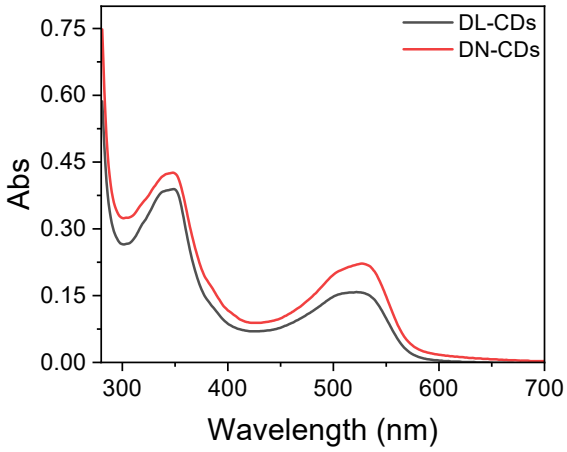

Fig. S2 UV-vis absorption of DL-CDs and DN-CDs (0.003 mg mL^{-1}).

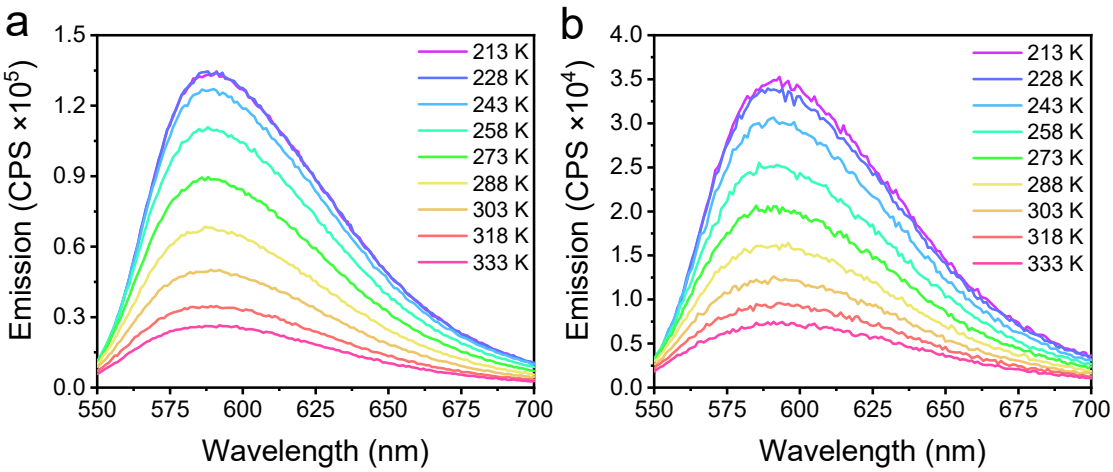

Fig. S3 Temperature dependence PL spectra of (a) DL-CDs and (b) DN-CDs (λ_{ex}=530 nm, 0.03 mg mL^{-1}).

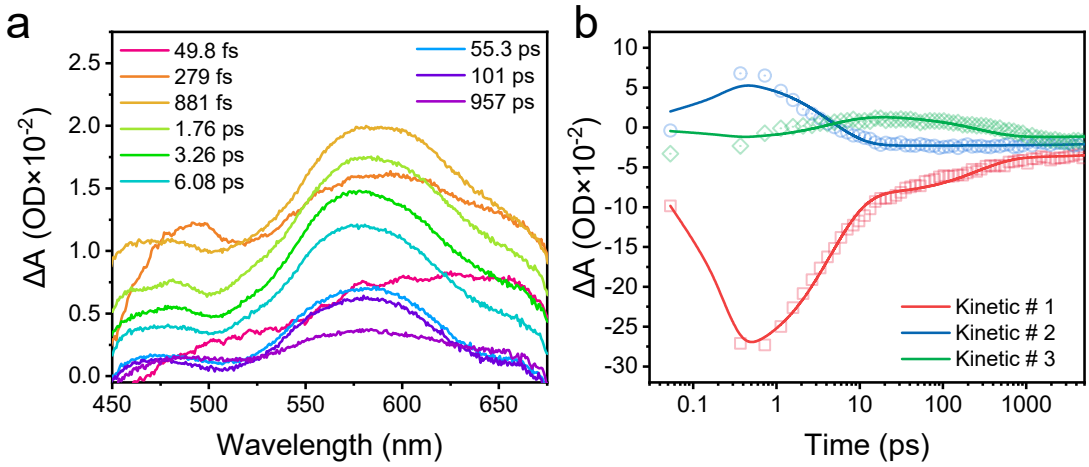

Fig. S4 Transient absorption spectra (a) and global fitting (b) of DL-CDs, λ_{ex}=300 nm, 0.03 mg mL^{-1}.

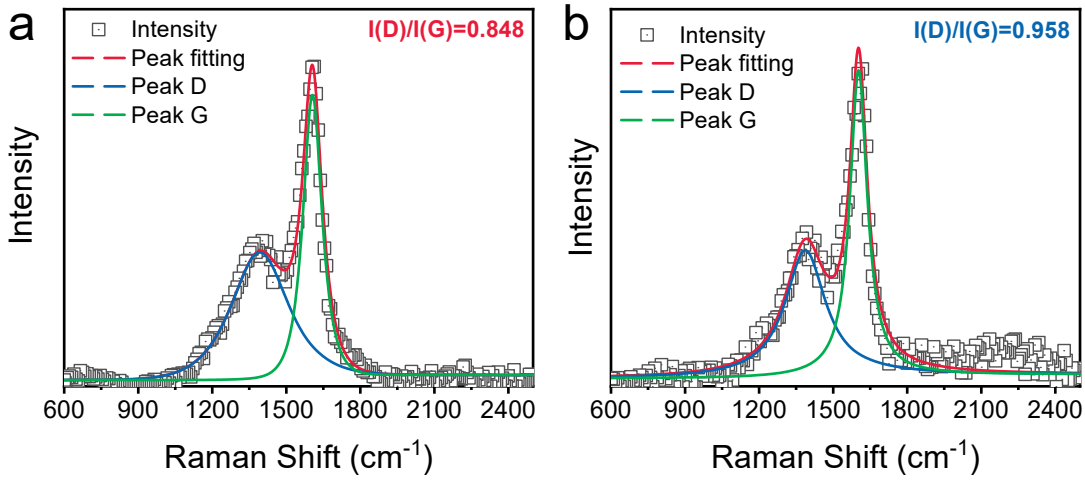

Fig. S5 Raman spectra of (a) DL-CDs and (b) DN-CDs.

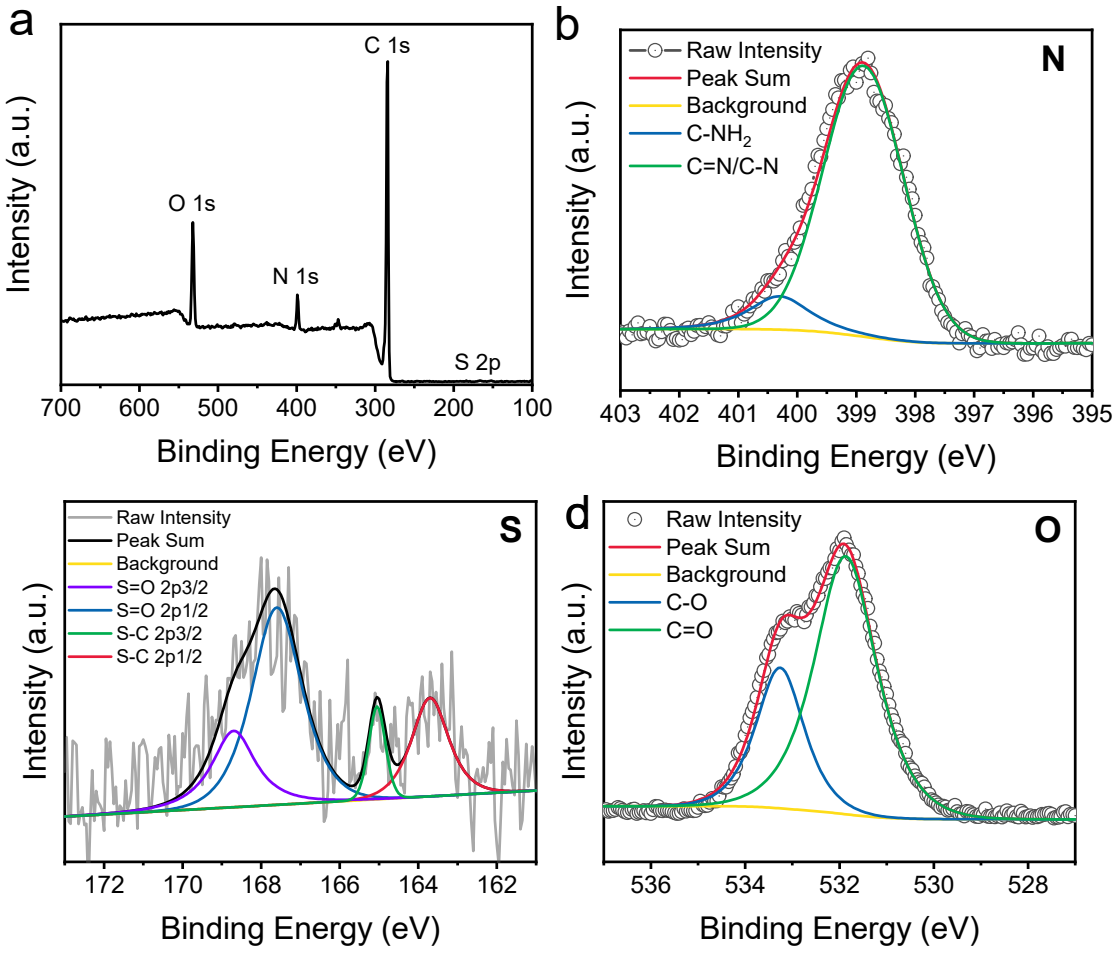

Fig. S6 (a) XPS spectrum and high-resolution energy spectra of (b) N1s, (c) S2p, and (d) O1s for DL-CDs.

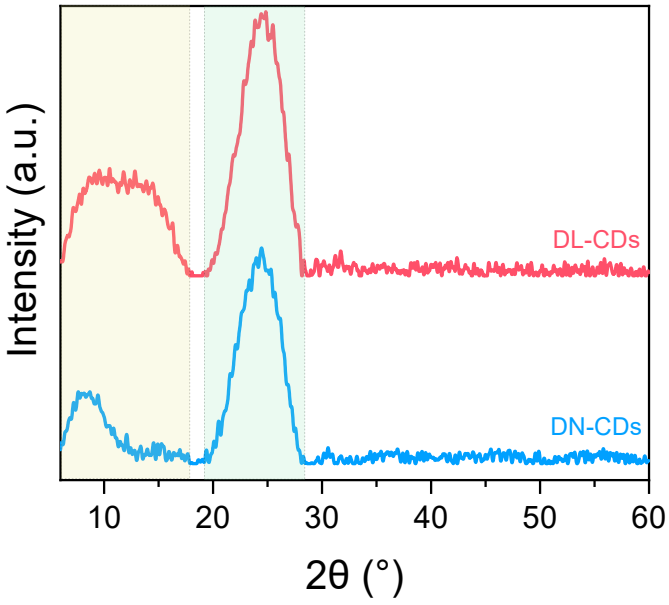

Fig. S7 XRD pattern of DL-CDs and DN-CDs

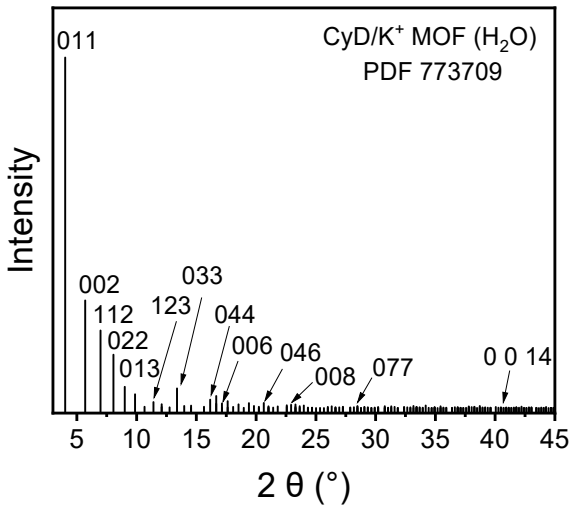

Fig. S8 XRD of CK-MOF, data comes from cif reported by Stoddart's group (*Angew. Chem. Int. Ed.*, 2010, 49, 8630).

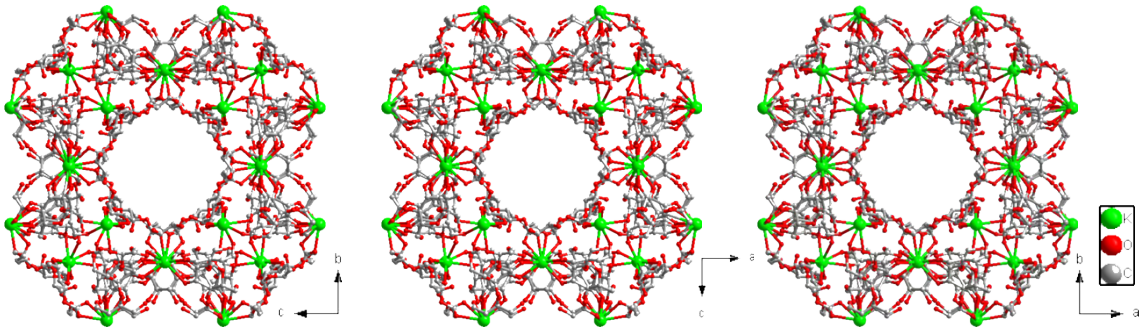

Fig. S9 Single crystal structure of CK-MOF from different perspectives, data comes from cif reported by Stoddart's group (*Angew. Chem. Int. Ed.*, 2010, 49, 8630).

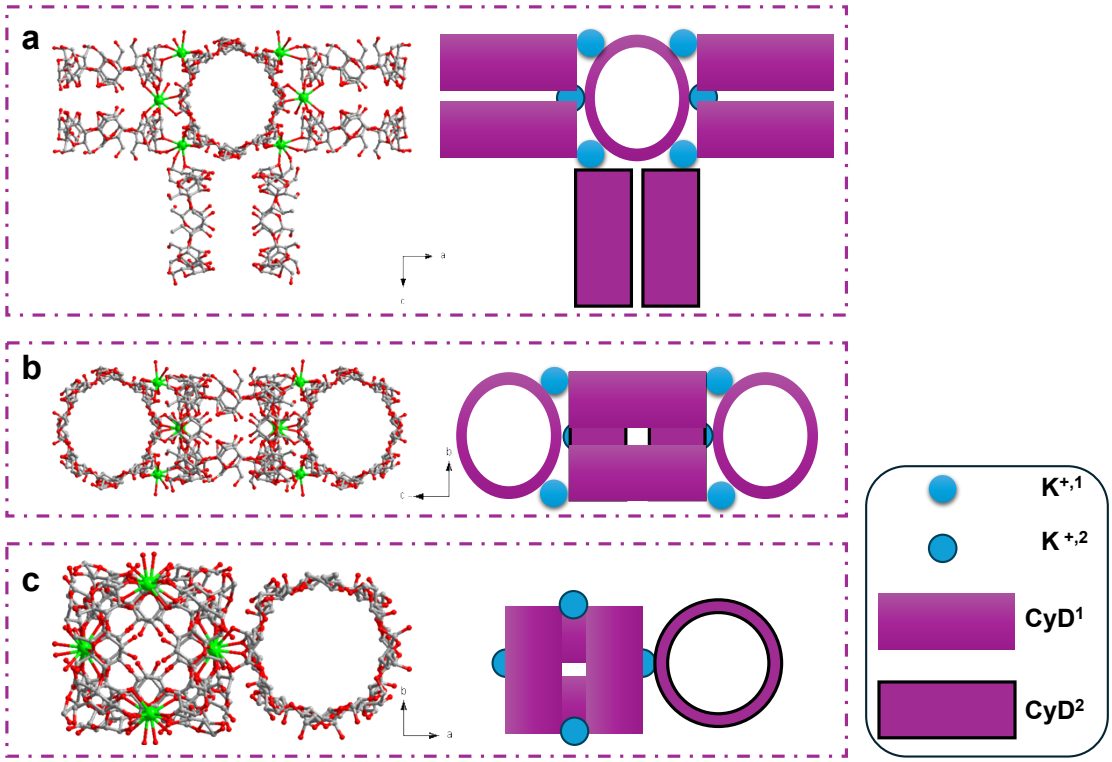

Fig. S10 Single crystal structure of *i*CK-MOF from different perspectives, the schematic diagram on the right represents a simplified molecular arrangement form.

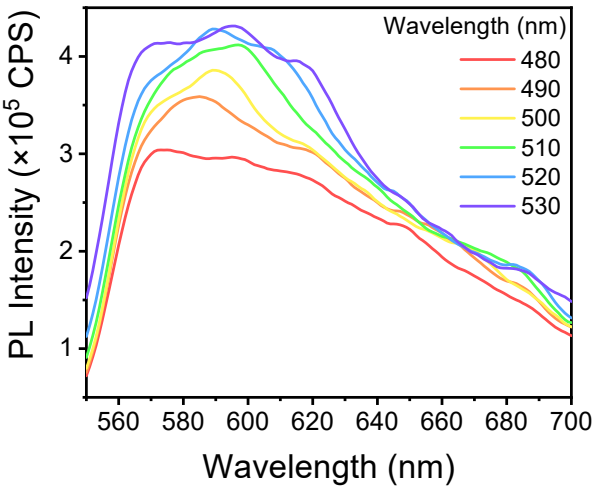

Fig. S11 PL spectra of CDs@*i*CK-MOF under different excitations.

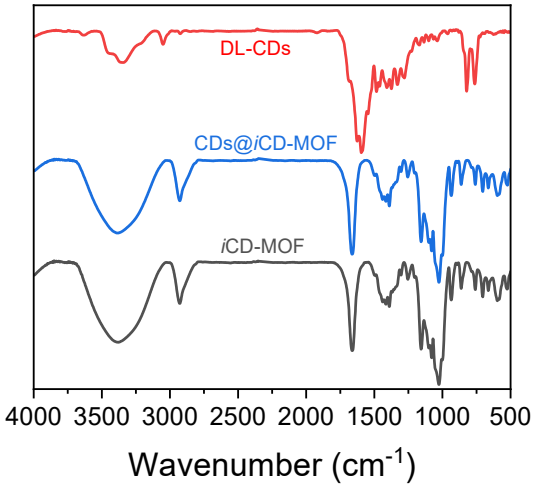

Fig. S12 FTIR of DL-CDs, CDs@*i*CK-MOF and *i*CK-MOF.

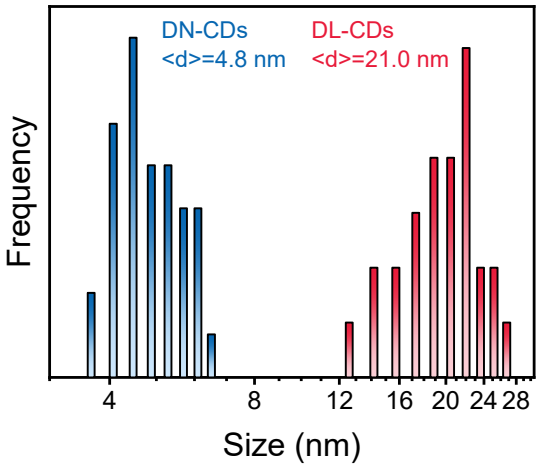

Fig. S13 Particle size distribution of DL-CDs and DN-CDs obtained from TEM images.